Effect of strain on the thermal conductivity of solids

Cite as: J. Chem. Phys. **125**, 164513 (2006); https://doi.org/10.1063/1.2361287
Submitted: 15 May 2006 . Accepted: 18 September 2006 . Published Online: 30 October 2006

Somnath Bhowmick, and Vijay B. Shenoy

Effect of strain on the thermal conductivity of solids

Somnath Bhowmick[a] and Vijay B. Shenoy[b]
Materials Research Center, Indian Institute of Science, Bangalore 560 012, India
and Centre for Condensed Matter Theory, Indian Institute of Science, Bangalore 560 012, India

(Received 15 May 2006; accepted 18 September 2006; published online 30 October 2006)

We present a systematic study of the effect of strain (equivalent to uniform pressure) on the thermal conductivity of an insulating solid. Following a theoretical analysis that uncovers the dependence of the thermal conductivity on temperature and strain, we present classical molecular dynamics calculations of the thermal conductivity. We find that the molecular dynamics results closely match the theoretical result. © *2006 American Institute of Physics*. [DOI: 10.1063/1.2361287]

I. INTRODUCTION

Materials modeling, aimed at understanding and designing materials with desired properties, is fast becoming a viable and fruitful method due to the rapid progress in computing technology.[1] In particular, modeling aimed at the theoretical prediction of transport properties of solids is important both from the point of view of applications and scientific interest. The endeavor to model transport properties continues to be challenged by the presence of multiple scales, both spatial and temporal,[1] and it is here that techniques such as molecular dynamics used in conjunction with parallel computing technology that have enabled the accurate theoretical evaluation of transport properties. The focus of this paper is a transport property—the thermal conductivity.

The theoretical modeling of thermal conductivity is useful for several applications. In particular, the efficient designing of devices at the microscale and nanoscale can be aided by a reliable predictive tool for thermal conductivity. For example, multilayer ceramic capacitors, designed for high frequency power switching device applications,[2] require fast heat dissipation (i.e., high thermal conductivity) for reliable operation. On the other hand, proper optimization is needed to get maximum electrical conductivity along with minimum thermal conductivity in the case of thermoelectric devices.[3] Efficiency of the small scale devices depends on the efficiency of the thermal management. Nanoscale devices, particularly thin films, usually contain residual strain after fabrication,[4,5] which may considerably affect the thermal transport properties of the material and the device concerned. Another area where strain (or equivalently pressure) has a strong influence on transport properties is found in geophysics. The materials at the core and mantle of the Earth are under high pressure and the determination of the transport properties by experiments is unfeasible, and computer modeling[6–9] has to be resorted to. Our work, which deals with the theoretical modeling of the dependence of the thermal conductivity on strain, is therefore important to understanding phenomena from the small scales (nanophysics) to those at the terrestrial scales.

In general, the net thermal conductivity of a solid arises from two distinct contributions. First is due to phonons and second is due to electrons. For an insulating solid, which is our focus, electrons are tightly bound to the atomic nuclei, and thermal current is carried solely by phonons. Further, two distinct types of parameters control effective thermal conductivity: thermodynamic parameters such as temperature and/or pressure, and "extrinsic" parameters such as impurities, defects, or bounding surfaces. Experimental as well as theoretical studies are available on the effect of temperature, pressure, and presence of defects on thermal conductivity.[10,11,14–21] However, to the best of our knowledge, a detailed study of the effect of strain (triaxial strain equivalent to the uniform pressure) comparing simple theories and molecular dynamics simulations is absent. The aim of this paper, therefore, is to understand the influence of strain on the lattice thermal conductivity (without defects, impurities, or surfaces). We do this by first considering the theoretical framework using the Peierls-Boltzmann formulation[12,13] to obtain a simple relation that determines the strain and temperature dependence of thermal conductivity. We then compute the thermal conductivity of a solid described by a simple empirical potential (Lennard-Jones potential for argon) using classical molecular dynamics via the Green-Kubo relations. Based on these calculations we suggest a simple empirical form for the strain/temperature dependence of conductivity.

The paper is organized as follows. In Sec. II we present the Peierls-Boltzmann formulation used to determine a simple analytical form for the strain dependence of the thermal conductivity. Section III contains the details of the interatomic potential and molecular dynamics simulations. The results of our simulations are presented and discussed in Sec. IV. We conclude the paper in Sec. V.

II. THEORY

In this section we develop simple analytical arguments to determine the strain dependence of the thermal conductivity following the formulation of Peierls.[12,13] The Hamiltonian (pertinent to the thermal conductivity calculation of our insulating monoatomic lattice) is given by

[a]Electronic mail: bsomnath@mrc.iisc.ernet.in
[b]Electronic mail: shenoy@mrc.iisc.ernet.in

$$H = \sum_{\mathbf{k}} \hbar\omega(\mathbf{k})\left(a_{\mathbf{k}}^{\dagger}a_{\mathbf{k}} + \frac{1}{2}\right) + \sum_{\mathbf{k}_1,\mathbf{k}_2,\mathbf{k}_3} \Gamma(\mathbf{k}_1,\mathbf{k}_2,\mathbf{k}_3) \times (a_{\mathbf{k}_1} + a_{\mathbf{k}_1}^{\dagger})(a_{\mathbf{k}_2} + a_{\mathbf{k}_2}^{\dagger})(a_{\mathbf{k}_3} + a_{\mathbf{k}_3}^{\dagger}), \quad (1)$$

where $\mathbf{k}$ is a phonon wave vector (we suppress the polarization index of the phonons for simplicity), $a_{\mathbf{k}}^{\dagger}$ and $a_{\mathbf{k}}$ are the associated phonon creation and annihilation operators, respectively, $\omega(\mathbf{k})$ is the frequency of the phonon mode $\mathbf{k}$, and Γ is the Fourier transform of the third order force constant matrix. As is well known, the last term allows for crystal momentum conserving Umklapp collisions of phonons that results in a finite thermal conductivity.

To obtain the thermal conductivity, the distribution function $n(\mathbf{k})$ is introduced[12,13] and differs from the equilibrium Bose distribution function $n^0(\mathbf{k}) = 1/(e^{\beta\omega(\mathbf{k})} - 1)$ ($\beta = 1/k_B T$, k_B—Boltzmann constant, and T—temperature). The distribution function $n(\mathbf{k})$ satisfies the (steady state) transport equation

$$\mathbf{v}(\mathbf{k}) \cdot \frac{\partial n}{\partial \mathbf{r}} = \left.\frac{\partial n}{\partial t}\right|_{\text{coll}}, \quad (2)$$

where $\mathbf{v}(\mathbf{k})$ is the group velocity of the phonon mode $\mathbf{k}$, and $\mathbf{r}$ is the position vector. The right hand side corresponds to the changes effected in the distribution function due to collisions which act to restore equilibrium. A standard approximation for the collision term is the relaxation time approximation

$$\left.\frac{\partial n}{\partial t}\right|_{\text{coll}} = -\frac{n - n^0}{\tau(\mathbf{k})}, \quad (3)$$

where $\tau(\mathbf{k})$ is the relaxation time for the phonon mode $\mathbf{k}$. The thermal conductivity tensor $\boldsymbol{\kappa}$ can now be readily evaluated as

$$\boldsymbol{\kappa} = \sum_{\mathbf{k}} \tau(\mathbf{k})\hbar\omega(\mathbf{k})\frac{\partial n^0(\mathbf{k})}{\partial T}\mathbf{v}(\mathbf{k})\mathbf{v}(\mathbf{k}) = \sum \tau(\mathbf{k})C(\mathbf{k})\mathbf{v}(\mathbf{k})\mathbf{v}(\mathbf{k}), \quad (4)$$

where $C(\mathbf{k})$ is the heat capacity (per unit volume) of the mode $\mathbf{k}$. At high temperatures (at temperatures larger than the Debye temperature) the heat capacity C is nearly constant, and the strain dependence of thermal conductivity is determined entirely by the strain dependence of the group velocity $\mathbf{v}$, and the relaxation time τ. We now proceed to evaluate the strain dependence, first for τ and then for $\mathbf{v}$.

To understand the strain dependence of the relaxation time, we define, following Peierls,[12]

$$\delta n = n - n^0 = \frac{n^0(n^0 + 1)}{k_B T}\zeta. \quad (5)$$

From a linearized solution of (2), we obtain

$$\zeta = -\tau(\mathbf{k})\mathbf{v}(\mathbf{k}) \cdot \nabla T \frac{\hbar\omega(\mathbf{k})}{T}. \quad (6)$$

The collision term in (2) can be evaluated from the Hamiltonian (1) using the Fermi golden rule[13] and the approximation (5) resulting in

$$\left.\frac{\partial n}{\partial t}\right|_{\text{coll}} = \int \frac{V d^3\mathbf{k}_1}{4\pi^2\hbar}\left(\frac{1}{2}W(\mathbf{k}_1 + \mathbf{k}_2 \to \mathbf{k})(n_1^0 + 1)(n_2^0 + 1)n^0(\zeta_1 + \zeta_2 - \zeta)\delta(\omega_1 + \omega_2 - \omega) + W(\mathbf{k}_1 + \mathbf{k} \to \mathbf{k}_3)(n_3^0 + 1)n_1^0 n^0 \times (\zeta_3 - \zeta_1 - \zeta)\delta(\omega_3 - \omega_1 - \omega)\right), \quad (7)$$

where V is the volume of the unit cell, $\mathbf{k}_2 = \mathbf{k} - \mathbf{k}_1 + \boldsymbol{G}$, $\mathbf{k}_3 = \mathbf{k} + \mathbf{k}_1 + \boldsymbol{G}$, where $\boldsymbol{G}$ is a reciprocal lattice vector, and $W(\mathbf{k}_1 + \mathbf{k}_2 \to \mathbf{k}) = |\Gamma(\mathbf{k}_1, \mathbf{k}_2, \mathbf{k})|^2$ (with a similar definition for $W(\mathbf{k}_1 + \mathbf{k} \to \mathbf{k}_3)$). We use the notation $f(\mathbf{k}_i) = f_i$ where f is any of n^0, ζ, $\mathbf{v}$, or ω. We can obtain an expression for the relaxation time by assuming it to be roughly independent of $\mathbf{k}$. To this end, we equate the relaxation time approximation for the collision integral (3), and that obtained from the Fermi golden rule (7). Assuming that the temperature gradient is in the x direction, we obtain

$$\frac{1}{\tau} \approx \int \frac{V d^3\mathbf{k}_1}{4\pi^2\hbar}\left(\frac{1}{2}W(\mathbf{k}_1 + \mathbf{k}_2 \to \mathbf{k})\left[\frac{(n_1^0 + 1)(n_2^0 + 1)n^0}{n^0(n^0 + 1)}\right] \times \left(\frac{(\omega_1\mathbf{v}_1 + \omega_2\mathbf{v}_2 - \omega\mathbf{v}) \cdot \mathbf{e}_x}{\omega\mathbf{v} \cdot \mathbf{e}_x}\right)\delta(\omega_1 + \omega_2 - \omega) + W(\mathbf{k}_1 + \mathbf{k} \to \mathbf{k}_3)\left[\frac{(n_3^0 + 1)n_1^0 n^0}{n^0(n^0 + 1)}\right] \times \left(\frac{(\omega_3\mathbf{v}_3 - \omega_1\mathbf{v}_1 - \omega\mathbf{v}) \cdot \mathbf{e}_x}{\omega\mathbf{v} \cdot \mathbf{e}_x}\right)\delta(\omega_3 - \omega_1 - \omega)\right). \quad (8)$$

We now consider temperatures greater than or equal to the Debye temperature of the solid (classical regime), thus $n^0(\mathbf{k}) \approx (n^0(\mathbf{k}) + 1) \approx k_B T/\hbar\omega(\mathbf{k})$, and the relaxation time reduces to

$$\frac{1}{\tau} \approx k_B T \int \frac{V d^3\mathbf{k}_1}{4\pi^2}\left(\frac{1}{2}W(\mathbf{k}_1 + \mathbf{k}_2 \to \mathbf{k})\left[\frac{\omega_1\omega_2}{\omega}\right] \times \left(\frac{(\omega_1\mathbf{v}_1 + \omega_2\mathbf{v}_2 - \omega\mathbf{v}) \cdot \mathbf{e}_x}{\omega\mathbf{v} \cdot \mathbf{e}_x}\right)\delta(\omega_1 + \omega_2 - \omega) + W(\mathbf{k}_1 + \mathbf{k} \to \mathbf{k}_3)\left[\frac{\omega_1\omega_3}{\omega}\right] \times \left(\frac{(\omega_3\mathbf{v}_3 - \omega_1\mathbf{v}_1 - \omega\mathbf{v}) \cdot \mathbf{e}_x}{\omega\mathbf{v} \cdot \mathbf{e}_x}\right)\delta(\omega_3 - \omega_1 - \omega)\right), \quad (9)$$

which will be used below to analyze the strain dependence of the thermal conductivity. We now introduce the dilation (we shall use the term "strain" to represent this quantity) ϵ with respect to a reference unit cell of volume V_0 defined as

$$\epsilon = \frac{V}{V_0}, \quad (10)$$

where, as defined above, V is the volume of the (possibly strained) unit cell. Clearly, $\epsilon < 1$ implies compressive strain, while $\epsilon > 1$ implies tensile strain. The phonon frequencies are expected to scale with strain as

$$\omega = \omega_0 \epsilon^{-a}, \tag{11}$$

where a is nonuniversal (potential dependent) number; for the type of potentials considered in this paper, this is a nonnegative number, i.e., the phonon "stiffens" with compressive strain. Note that $a=-(\partial \ln \omega)/(\partial \ln \epsilon)$ is the Grüneisen parameter. The result (11) may be seen by noting that $\omega \sim \phi''(r_\epsilon)$, where ϕ'' is the second derivative of the interatomic potential evaluated at the strained interatomic distance $r_\epsilon = \epsilon^{1/3} r_0$ (r_0 is the zero temperature interatomic separation). For potentials (of the Lennard-Jones type), $\phi''(r_\epsilon) \sim \epsilon^{-a}\phi''(r_0)$ (the leading dependence on ϵ), and (11) follows. Note that $\Gamma(\mathbf{k}_1,\mathbf{k}_2,\mathbf{k}_3)$ in (1) is the Fourier transform of the third order force constants of the lattice $g(i,j,k)$ (order of magnitude $g \sim \epsilon^b, b>0$) normalized by the phonon frequencies, i.e.,

$$\Gamma(\mathbf{k}_1,\mathbf{k}_2,\mathbf{k}_3) \sim \frac{g}{\sqrt{\omega_1\omega_2\omega_3}}. \tag{12}$$

Using the above relations in (9), we find that

$$\tau \sim \frac{1}{T}\epsilon^{-(2a+2b)}. \tag{13}$$

Noting now that $\mathbf{v} \sim \omega$, we see that the group velocity scales with strain in the same fashion as the phonon frequency. From (4) it follows that

$$\kappa \sim T^{-1}\epsilon^{-\gamma}, \tag{14}$$

where γ ($=4a+2b$, in the present analysis) is a potential (material) dependent exponent. This expression for the temperature/strain dependence of thermal conductivity will be useful in comparison with the molecular dynamics simulations described in the next section. The functional dependence on strain shown in (14) was proposed from the simulation results in Ref. 21.

III. MODEL AND MOLECULAR DYNAMICS DETAILS

In this section we describe the atomistic model used in our molecular dynamics (MD) calculations, the simulation details, and the details of calculation of the thermal conductivity.

A. Model

The interatomic potential used in our molecular dynamics calculations is the Lennard-Jones pair potential[24] given by

$$\phi(r_{ij}) = 4\varepsilon\left[\left(\frac{\sigma}{r_{ij}}\right)^{12} - \left(\frac{\sigma}{r_{ij}}\right)^{6}\right], \tag{15}$$

where r_{ij} is the distance between the atoms i and j. The values of the energy $\epsilon=0.0104$ eV and the distance $\sigma=3.405$ Å are chosen to be that of the argon[25] which is a system well studied by molecular dynamics, allowing us to compare our results with earlier work (wherever applicable). The pair potential is cut-off smoothly at distance $r_{cut}=2.5\sigma$.

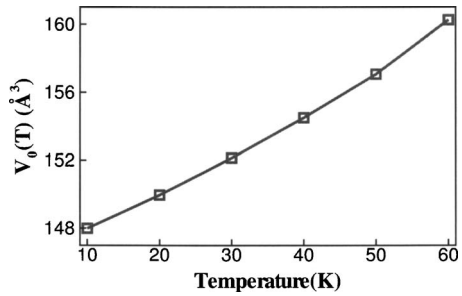

FIG. 1. Equilibrium (unstrained, zero pressure) unit cell volume at different temperatures.

B. Calculation of thermal conductivity

We calculate the thermal conductivity from the molecular dynamics trajectory by using the Green-Kubo relations[22,23]

$$\kappa = \frac{1}{3V_c k_B T^2}\int_0^\infty \langle \boldsymbol{j}(0)\cdot\boldsymbol{j}(t)\rangle dt, \tag{16}$$

where V_c is the volume of the simulation cell, $\boldsymbol{j}(t)$ is the microscopic heat current, and $\langle \boldsymbol{j}(0)\cdot\boldsymbol{j}(t)\rangle$ denotes the heat current autocorrelation function. Microscopic heat current $\boldsymbol{j}$ is defined as[26]

$$\boldsymbol{j}(t) = \sum_i E_i \boldsymbol{u}_i + \frac{1}{2}\sum_{i,j}(\boldsymbol{F}_{ij}\cdot\boldsymbol{u}_i)\boldsymbol{r}_{ij}, \tag{17}$$

where the sum is over all the particles in the system. E_i and $\boldsymbol{u}_i$ are, respectively, the total energy and velocity of ith particle at time t, and $\boldsymbol{F}_{ij}$ and $\boldsymbol{r}_{ij}$ are, respectively, the interparticle force and separation, respectively, between the ith and jth particles. Our simulation cell consists of $4\times4\times4$ fcc unit cells (i.e., 256 atoms) with periodic boundary conditions, which is known to be sufficient to eliminate the finite size effects on the calculated thermal conductivity.[10,11] The first step is the determination of the equilibrium lattice spacing at zero pressure, or equivalently the unstrained unit cell volume. This is achieved by a set of constant pressure/temperature (NPT) simulations at zero pressure and temperatures ranging from 10 to 60 K. Equilibrium value of the unit cell volume as a function of temperature thus determined, is plotted in Fig. 1.

The unstrained (zero pressure) unit cell volume $V_0(T)$ (with an associated lattice parameter) shown in Fig. 1 at a given temperature is taken as the reference state at that temperature. Strain ϵ is applied to the atomistic simulation cell by rescaling the size of the periodic box to $V=\epsilon V_0(T)$. Furthermore, the positions of all atoms in the box are also rescaled via $\boldsymbol{r}\rightarrow\epsilon^{1/3}\boldsymbol{r}$. This achieves a homogeneous triaxial state of deformation with respect to the reference state. At each temperature, and for each strain level [ranging from $\epsilon=0.9$ (compressive) to $\epsilon=1.1$ (tensile)], constant volume/energy (NVE) simulations are carried out to obtain the heat current $\boldsymbol{j}$ as a function of time.

For all the molecular dynamics runs, we have chosen the integration time step to be 0.001 ps which is known to be sufficient to resolve the phenomena of interest.[10,11] Initially we run the constant volume/temperature simulation for suf-

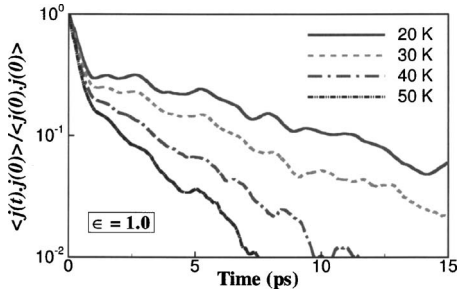

FIG. 2. The heat current autocorrelation function at four different temperatures, showing two stage decay. In an unstrained lattice the first sharp decay is (essentially) independent of temperature and is followed by a slow long range one, decaying at a faster rate with increasing temperature. The fluctuation of heat current in equilibrium dies much faster at higher temperatures and corresponding κ decreases. See also Figs. 4 and 5.

ficient time (of the order of 10^5 time steps) to attain equilibrium and subsequently another 10^6 time steps to obtain the heat current autocorrelation function. Thermal conductivity is calculated by integrating (16) numerically. We average the results for thermal conductivity over ten independent simulations, each with a different random initial configuration, for every temperature and strain.

IV. RESULTS AND DISCUSSION

Typical normalized heat current autocorrelation functions obtained from our simulations are illustrated in Figs. 2 and 3 for different temperatures (unstrained) and strains (temperature of 40 K), respectively. All the curves follow a two stage decay and can be fitted to a sum of double exponential function,[11,15]

$$\frac{\langle \boldsymbol{j}(t)\cdot\boldsymbol{j}(0)\rangle}{3} = A\exp(-t/\tau_1) + A_2\exp(-t/\tau_2), \tag{18}$$

where A's are constants and τ's are the characteristic decay times of fluctuation of the heat current in equilibrium. We record the values of τ_1 and τ_2 at different temperatures (unstrained) and strains (fixed temperature of 40 K) in Tables I and II, respectively. The relaxation time τ_1 is due to the "short wavelength" phonons and is usually an order of magnitude smaller than τ_2 which is attributed to the long wavelength phonons.[11] Interestingly, both temperature and strain do not affect τ_1 significantly, while τ_2 is a strong function of both temperature and strain. It is clear, therefore, that dominant contribution to the temperature and strain dependence of the thermal conductivity arises from the long wavelength phonons. As expected from (13), τ_2 decreases with increasing temperature, and τ_2 decreases on going from compressive strains to tensile strains (see Table I and II).

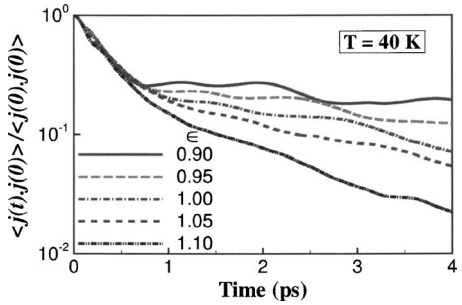

FIG. 3. The heat current autocorrelation function for different strains at 40 K, showing two stage decay. The first sharp decay is independent of strain. The second long-time decay is faster as we move from compressive to tensile strains and corresponding κ decreases. See also Figs. 4 and 7. Strains with $\epsilon = V/V_0(T) < 1$ are compressive and $V/V_0(T) > 1$ are tensile, where V is the volume of the strained unit cell and $V_0(T)$ is the volume of the unstrained unit cell at temperature T.

TABLE I. Phonon lifetime at different temperatures (unstrained) in solid argon. τ_1 and τ_2 are the two characteristic decay times of the heat current autocorrelation function defined in (18). τ_{av} is the average decay time defined by (24)

Temperature (K)	τ_1 (ps)	τ_2 (ps)	τ_{av} (ps)
10	0.285	21.965	7.001
20	0.265	8.401	3.665
30	0.267	5.115	2.111
40	0.274	3.225	1.500
50	0.265	2.226	1.123
60	0.263	1.998	0.997

The thermal conductivity calculated using (16) and (18) is plotted as a function of strain and temperature in Fig. 4. The thermal conductivity monotonically decreases with increasing temperature (see also Fig. 5). Further, the thermal conductivity monotonically decreases with strain going from compressive to tensile. Motivated by our theoretical estimation of the thermal conductivity (14), we fit the data shown in Fig. 4 to a function of the form

$$\kappa = +AT^{-\alpha}\left(\frac{V}{V_0(T)}\right)^{-\gamma}, \tag{19}$$

where A, α, and γ are constants, and $V_0(T)$ (see Fig. 1) and V are, respectively, the equilibrium (unstrained) volume and volume of the strained lattice at absolute temperature T. We find that the best fit values of A, α, and γ for our Lennard-Jones system are 4.61, 1.45, and 9.59, respectively [the units of κ is W/(m K) and that of T is K].

We note that the exponent α in (19) is different from unity as predicted by the analysis of Sec. II [see (14)]. Our analysis is based on "three-phonon" processes. It is well known that "four-phonon" processes also contribute as

TABLE II. Phonon lifetime at different strains (fixed temperature of 40 K) in solid argon. τ_1 and τ_2 are the two characteristic decay times of heat current autocorrelation function [see (18)]. τ_{av} is the average decay time defined by (24). V and V_0 are, respectively, the strained and unstrained volumes of the unit cell at temperature T=40 K.

$\epsilon = V/V_0$ (40 K)	τ_1 (ps)	τ_2 (ps)	τ_{av} (ps)
0.900	0.219	5.169	1.801
0.925	0.222	4.426	1.650
0.950	0.258	4.326	1.611
0.975	0.269	3.886	1.573
0.000	0.274	3.225	1.500
1.025	0.288	3.165	1.452
1.050	0.301	2.443	1.416
1.075	0.310	2.409	1.370
1.100	0.283	1.856	1.351

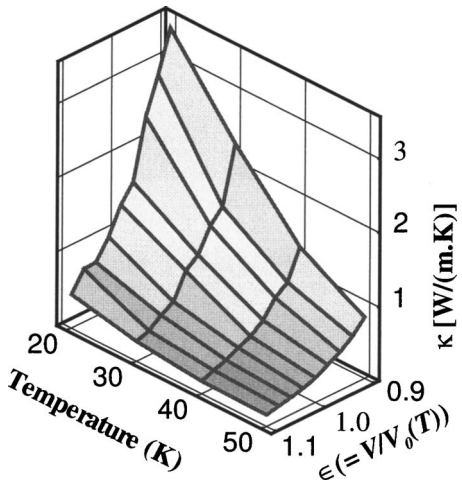

FIG. 4. Thermal conductivity [determined from molecular dynamics calculations via (16)] as a function of temperature and strain.

pointed out by Pomaranchuk,[12] and accounting for this provides that $1 \leqslant \alpha \leqslant 2$. The value of $\alpha = 1.45$ is within this limit. The strain dependence found in our MD simulations is entirely as predicted by (14). Clearly, γ is dependent on the interatomic potential.

We now present further analysis of our results. For an isotropic solid (4) reduces to

$$\kappa = \tfrac{1}{3} C v^2 \tau, \tag{20}$$

where C, v, and τ are heat capacity per unit volume, speed of sound, and relaxation time of phonons, respectively. This result, which we shall call the "kinetic theory" (KT) result, will be used in the discussion below. The high temperature (classical) heat capacity of the phonons is independent of temperature, and thus the thermal conductivity can be estimated [alternative to (16)] using (20). To this end we determine the temperature and strain dependence of v and τ. We estimate the speed of sound v by averaging over the longitudinal and transverse sound velocities, v_l and v_t, respectively,

$$v = \left[\frac{1}{3} \left(\frac{1}{v_l^3} + \frac{2}{v_t^3} \right) \right]^{-1/3}. \tag{21}$$

Longitudinal and transverse sound velocities are calculated via[27]

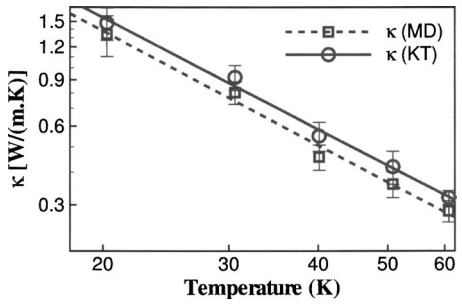

FIG. 5. Comparison of κ calculated from MD [see (16)] and KT [see (20)] at different temperatures for the unstrained solid. The error bars are standard deviations over results of ten independent simulations each with a different initial random configuration.

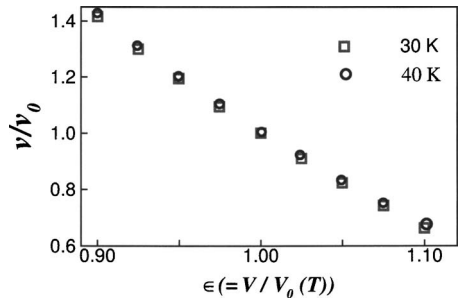

FIG. 6. Strain dependence of the normalized sound velocity (21). Velocity of sound decreases with increasing tensile strain (i.e., increasing volume). v_0 corresponds to sound velocity in an unstrained crystal at the temperature indicated.

$$v_l^2 = \tilde{c}_{11}/\rho, \tag{22}$$

$$v_t^2 = \tilde{c}_{44}/\rho, \tag{23}$$

where $\tilde{c}$'s are the elastic constants and ρ is the density of the solid. Figure 6 exhibits the strain dependence of normalized sound velocities at different temperatures, where v_0 stands for the sound velocity in the unstrained crystal at different temperatures. We note that the sound velocity is calculated by accounting for both the thermal expansion and the strain in the determination of the elastic constants (calculated using the quasiharmonic approximation following Ref. 28) and the density. Calculation of the phonon relaxation time is not as straightforward. As is evident from (18), fluctuations of heat current in equilibrium decay in two stages and with two characteristic decay times, both contributing to the thermal conductivity, although the main contribution arises from the long wavelength phonons. An average decay time can still be defined as[29]

$$\tau_{\mathrm{av}} = \frac{3 V_c \kappa k_B T^2}{\langle \boldsymbol{j}(0) \cdot \boldsymbol{j}(0) \rangle}, \tag{24}$$

where κ is the thermal conductivity calculated from the heat current autocorrelation function using (16). We substitute the values of τ_{av} (see Tables I and II) for the phonon relaxation times and the velocity of sound calculated using (21) in (20) to obtain a second estimate of the thermal conductivity. Figures 5 and 7 show the comparison of thermal conductivity calculated from the MD and KT at different temperatures and strains. These two results are in excellent agreement (within

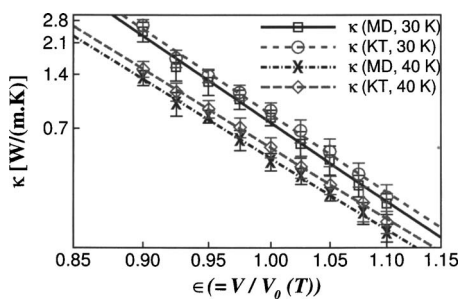

FIG. 7. Comparison of κ computed from MD [see (16)] and KT [see (20)] at different strains and temperatures. The error bars have been calculated by averaging κ over ten independent simulations, each with a different initial seed velocity and taking the standard deviation.

5%) with each other. This analysis shows that the strain dependence of the thermal conductivity arises from both the change of the speed of sound and the dependence of the relaxation time on strain (both of which monotonically decreases when strain goes from compressive to tensile). This is, yet again, as anticipated in our derivation of (14).

Prior to the conclusion of the paper, we comment on the values on thermal conductivities obtained from our simulations. It is known[30] that the Lennard-Jones potential with a cutoff of 2.5σ (which is what we use in this paper) underestimates (by roughly a factor of 2) the experimental thermal conductivity of argon. However, a careful study[10] of the same system including the long range energy corrections obtains values that are within 20% of the experiment, while the qualitative features of temperature dependence, etc., remain unaltered. Another study of argon[11] with a cutoff of 3.1σ (without long range energy corrections) estimates values of thermal conductivity (in an unstrained crystal) which are within 30%–40% of the experimental values. Our values are a few percentage smaller (in the unstrained crystal) than those of Ref. 11, possibly due to a slightly different lattice parameter [the lattice parameter of Ref. 11 (5.24 Å) is smaller than that of ours (5.26 Å)] owing to the different cutoffs.

V. CONCLUSION

In this paper we have presented a systematic study of the temperature and strain dependence of thermal conductivity of insulating solids. Our theoretical analysis used the Fermi golden rule to determine the temperature and strain dependence of the phonon relaxation time, and a power law scaling relationship of thermal conductivity on the temperature and strain is found. We performed classical molecular dynamics simulations and obtained the strain and temperature dependence of the thermal conductivity. We find that the thermal conductivity from molecular dynamics matches the form suggested by the theory. Further, our analysis showed how strain affects thermal conductivity—first by the change of the velocity of sound, and second via the relaxation time. This may be contrasted with the effect of temperature which affects (essentially) only the relaxation time.

As noted in the Introduction the study of strain effects on thermal conductivity has many applications from nanoscales to geophysical scales. We are presently investigating the effect of strain on the thermal conductivity of nanostructures and shall report our findings in a future publication.

ACKNOWLEDGMENT

Support for this work by BRNS, India is gratefully acknowledged.

[1] R. Phillips, *Crystals, Defects and Microstructures, Modelling Across Scales* (Cambridge University Press, Cambridge, 2001).
[2] Y. Sakabe, M. Hayashi, T. Ozaki, and J. P. Canner, *Electronic Components and Technology Conference* (IEEE, New York, 1995), p. 234.
[3] G. Chen and A. Shakouri, J. Heat Transfer **124**, 242 (2002).
[4] M. Adamcyk, J. H. Schmid, and T. Tiedje, Appl. Phys. Lett. **80**, 4357 (2002).
[5] S. G. Malhotra, Z. U. Rek, S. M. Yalisove, and J. C. Bilello, J. Appl. Phys. **79**, 6872 (1996).
[6] M. Matsui and G. D. Price, Nature (London) **351**, 735 (1991).
[7] R. E. Cohen, Phys. Rev. B **50**, 12301 (1994).
[8] I. Inbar and R. E. Cohen, Geophys. Res. Lett. **22**, 1533 (1995).
[9] S.-N. Luo, T. Cagin, A. Strachan, W. A. Goddard III, and T. J. Ahrens, Earth Planet. Sci. Lett. **202**, 147 (2002).
[10] K. V. Tretiakov and S. Scandolo, J. Chem. Phys. **120**, 3765 (2004).
[11] A. J. H. McGhughey and M. Kaviany, Int. J. Heat Mass Transfer **47**, 1783 (2004).
[12] R. E. Peierls, *Quantum Theory of Solids* (Oxford University Press, London, 1956).
[13] E. M. Lifshitz and L. P. Pitaevskii, *Physical Kinetics* (Butterworth Heinemann, Oxford, 1995).
[14] F. Clayton and D. N. Batchelder, J. Phys. C **6**, 1213 (1973).
[15] J. Che, T. Cagin, W. Deng, and W. A. Goddard III, J. Chem. Phys. **113**, 6888 (2000).
[16] D. P. White, J. Nucl. Mater. **212**, 1069 (1994).
[17] K. C. Sood and M. K. Roy, J. Phys.: Condens. Matter **5**, 301 (1993).
[18] J. Li, L. Porter, and S. Yip, J. Nucl. Mater. **255**, 139 (1998).
[19] D. G. Cahill and R. O. Pohl, Solid State Commun. **70**, 927 (1989).
[20] P. Jund and R. Jullien, Phys. Rev. B **59**, 13707 (1999).
[21] K. V. Tretiakov and S. Scandolo, J. Chem. Phys. **121**, 11177 (2004).
[22] M. S. Green, J. Chem. Phys. **22**, 398 (1954).
[23] R. Kubo, J. Phys. Soc. Jpn. **12**, 570 (1957).
[24] M. P. Allen and D. J. Tildesley, *Computer Simulation of Liquids* (Clarendon, Oxford, 1987).
[25] N. W. Ashcroft and N. D. Mermin, *Solid State Physics* (Brooks-Cole, Belmont, MA, 1976).
[26] D. A. McQuarrie, *Statistical Mechanics* (Harper & Row, New York, 1976).
[27] G. Leibfried and W. Ludwig, *Solid State Physics* (Academic, New York, 1961), Vol. 12, p. 275.
[28] V. Shenoy, V. Shenoy, and R. Phillips, Mater. Res. Soc. Symp. Proc. **538**, 465 (1999).
[29] S. Volz, J. B. Saulnier, M. Lallemand, B. Perrin, P. Depondt, and M. Mareschal, Phys. Rev. B **54**, 340 (1996).
[30] H. Kaburaki, J. Li, and S. Yip, Mater. Res. Soc. Symp. Proc. **538**, 503 (1999).